QUARTERLY OF APPLIED MATHEMATICS

Vol. XXVII OCTOBER 1969 No. 3

NUMERICAL STUDY OF QUADRATIC AREA-PRESERVING MAPPINGS*

BY

M. HÉNON

C.N.R.S., Institut d'Astrophysique, Paris

Abstract. Dynamical systems with two degrees of freedom can be reduced to the study of an area-preserving mapping. We consider here, as a model problem, the mapping given by the quadratic equations: $x_1 = x \cos \alpha - (y - x^2) \sin \alpha$, $y_1 = x \sin \alpha + (y - x^2) \cos \alpha$, which is shown to be in a sense the simplest nontrivial mapping. Some analytical properties are given, and numerical results are exhibited in Figs. 2 to 14.

1. Introduction. Many important problems in physics can be reduced to the study of a conservative dynamical system with two degrees of freedom. Let us mention, for example, the restricted problem of three bodies in astronomy [1, 2]; the motion of a star in an axisymmetric galaxy [3]; the motion of a satellite around an oblate planet [4]; the oscillations of a satellite [5]; the motion of charged particles trapped in the earth's magnetic field [6]; the orbits of particles in accelerators and in mirror machines [7, 8]; the motion of coupled nonlinear oscillators, etc.

It is well known [9] that the study of a conservative dynamical system with two degrees of freedom can be reduced to the study of a plane area-preserving mapping by the introduction of a *surface of section*. This reduction has often been used in theoretical work, and also in many of the physical problems mentioned above. It is a very striking fact that, although these problems are quite different, the results are rather similar in their general features. The same features have been found also in numerical experiments with a mapping which was not connected with any particular application [3]. Thus there is a strong suggestion that the observed features are common to all dynamical problems with two degrees of freedom (with the exception of some particular cases, such as integrable systems) and also to all area-preserving mappings (also excluding some particular cases).

It appears then worthwhile to consider more fully a model problem, which should of course be chosen as simple as possible, while still retaining the properties of the general case. This is the purpose of the present paper. It turns out that the simplest useful model is a mapping where the transformation formulas are second-degree polynomials in cartesian coordinates. This mapping will be studied here mostly by numerical computations.

2. The mapping. We seek an area-preserving mapping of the (x, y) plane over itself, defined by

*Received August 28, 1967; revised version received July 20, 1968.

$$x_1 = f(x, y), \qquad y_1 = g(x, y). \tag{1}$$

It is well known that a central role is played by the points which are invariant in the mapping, and stable in the linear approximation [2] (we shall always use the words "stable" and "unstable" with this meaning). Therefore we shall assume that the origin $x = y = 0$ is such a stable invariant point.

For numerical studies it is simplest to have polynomials for f and g. In that case the mapping is called an "entire Cremona transformation", and it has also the advantage that a number of theoretical results are available [19, 20, 21]. Thus the simplest example we can imagine is one where f and g are linear functions of x and y. Then, by an appropriate linear change of coordinates [10], the mapping can be reduced to the form

$$x_1 = x \cos \alpha - y \sin \alpha, \qquad y_1 = x \sin \alpha + y \cos \alpha, \tag{2}$$

where α is a constant. This is simply a rotation of angle α around the origin. Such a mapping has only trivial properties and is not representative of the general case.

Let us try next second-degree polynomials for f and g:

$$\begin{aligned} x_1 &= ax + by + cx^2 + dxy + ey^2, \\ y_1 &= a'x + b'y + c'x^2 + d'xy + e'y^2. \end{aligned} \tag{3}$$

Again, if the origin is a stable invariant point, this mapping can be reduced by a linear change of coordinates to a simpler form

$$\begin{aligned} x_1 &= x \cos \alpha - y \sin \alpha + cx^2 + dxy + ey^2, \\ y_1 &= x \sin \alpha + y \cos \alpha + c'x^2 + d'xy + e'y^2. \end{aligned} \tag{4}$$

The area-preserving condition is

$$\partial(x_1 , y_1)/\partial(x, y) = 1 \tag{5}$$

and imposes the following relations between the coefficients:

$$\begin{aligned} (d' + 2c) \cos \alpha + (2c' - d) \sin \alpha &= 0, \\ (d + 2e') \cos \alpha + (d' - 2e) \sin \alpha &= 0, \\ cd' - c'd &= 0, \\ ce' - c'e &= 0, \\ de' - d'e &= 0. \end{aligned} \tag{6}$$

Using these conditions and additional linear changes of coordinates, we shall try to reduce the mapping (4) to the simplest possible form. The last three conditions (6) show that the second-degree terms in the two equations (4) must be proportional. The coefficients can then be written

$$\begin{aligned} c &= C \sin \beta, \qquad & d &= D \sin \beta, \qquad & e &= E \sin \beta, \\ c' &= C \cos \beta, \qquad & d' &= D \cos \beta, \qquad & e' &= E \cos \beta, \end{aligned} \tag{7}$$

where C, D, E, β are new constants. The first two conditions (6) become

$$\begin{aligned} 2C \sin (\alpha + \beta) + D \cos (\alpha + \beta) &= 0, \\ D \sin (\alpha + \beta) + 2E \cos (\alpha + \beta) &= 0. \end{aligned} \tag{8}$$

We effect now the following linear change of coordinates:

$$x' = -(C+E)[x \cos(\alpha+\beta) - y \sin(\alpha+\beta)],$$
$$y' = -(C+E)[x \sin(\alpha+\beta) + y \cos(\alpha+\beta)]. \tag{9}$$

Substituting into (4), and taking into account the relations (7) and (8), we find easily that the mapping becomes

$$x_1' = x' \cos\alpha - y' \sin\alpha + x'^2 \sin\alpha,$$
$$y_1' = x' \sin\alpha + y' \cos\alpha - x'^2 \cos\alpha. \tag{10}$$

Only one parameter is left: α, instead of the ten coefficients of (3). This last parameter cannot be eliminated, because it is the rotation angle in the first-order approximation, and this angle is known to be characteristic of the mapping and invariant under any change of coordinates.

We can rewrite (10), suppressing the primes for convenience, as

$$x_1 = x\cos\alpha - (y - x^2)\sin\alpha,$$
$$y_1 = x\sin\alpha + (y - x^2)\cos\alpha, \tag{11}$$

and it is then obvious that this mapping T is the product of two simpler mappings: $T = RS$, where S is a shearing parallel to the y axis:

$$x_{1/2} = x, \qquad y_{1/2} = y - x^2, \tag{12}$$

and R is a rotation:

$$x_1 = x_{1/2}\cos\alpha - y_{1/2}\sin\alpha, \qquad y_1 = x_{1/2}\sin\alpha + y_{1/2}\cos\alpha. \tag{13}$$

S and R are separately area-preserving. In fact, it has been shown by Engel [19], [20] that any polynomial area-preserving mapping can be reduced to a similar form.

The mapping T, expressed by Eqs. (11), is the one which we shall adopt for study. It has the following advantages:

1. As we shall see later, it exhibits all the typical properties of more complicated mappings and dynamical systems.
2. It is the simplest nontrivial case, as we have seen. The simplicity of the expressions (11) makes them very well suited for numerical experiments, and also for theoretical analysis (see [11]).
3. The study of this mapping has been suggested by Siegel [12].
4. It has some generality, since all second-degree area-preserving mappings can be reduced to this form by a linear change of coordinates.
5. It contains a parameter α, so that we have in effect a one-parameter family of mappings. Instead of considering just one value of α, we shall scan systematically the whole family; this will provide us with a variety of situations, and will also reveal many interesting phenomena which appear only in a restricted range of values of α.
6. The position and the stability of all the invariant points of T, T^2, T^3, T^4 can be computed exactly, as we shall see. These points play a very important role in the mapping.
7. The inverse mapping T^{-1} is given by formulas as simple as those of T itself; in fact, T^{-1} is the symmetrical of T with respect to a given axis, as we shall show.

3. Some properties. a. From (11) we easily derive the formulas for the inverse transformation T^{-1}, either by direct computation or by using $T^{-1} = S^{-1}R^{-1}$:

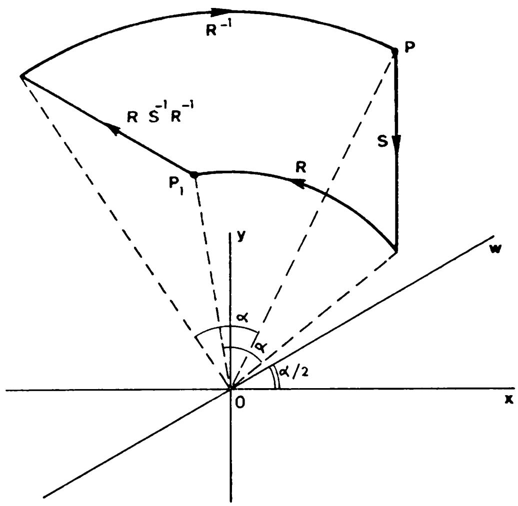

FIG. 1. Geometrical interpretation of the mapping $T = RS$ and its inverse.

$$\begin{aligned} x &= x_1 \cos\alpha + y_1 \sin\alpha, \\ y &= -x_1 \sin\alpha + y_1 \cos\alpha + (x_1 \cos\alpha + y_1 \sin\alpha)^2. \end{aligned} \tag{14}$$

Thus we have the remarkable property that T^{-1} is also a quadratic mapping. (Engel [19] has shown that in general the inverse of a polynomial area-preserving mapping is also a polynomial area-preserving mapping.) We can also write

$$T^{-1} = R^{-1}(RS^{-1}R^{-1}) \tag{15}$$

and remark that $RS^{-1}R^{-1}$ is a shearing deduced from S by a symmetry with respect to an axis $0w$ which makes an angle $\alpha/2$ with the $0x$ axis (Fig. 1). R^{-1} can be deduced from R by the same symmetry. This shows that T^{-1} is the mapping symmetrical of T with respect to the axis $0w$. In other words, if we denote by P^* the symmetrical of a point P with respect to $0w$, there is:

$$T^{-1}(P^*) = [T(P)]^*. \tag{16}$$

In what follows, we shall be interested in sets of points obtained by repeated application of the mapping:

$$P_0, P_1 = T(P_0), \cdots, P_n = T(P_{n-1}) = T^n(P_0). \tag{17}$$

For any such set of points there exists a symmetrical set, obtained by starting from P_n^* and applying n times the mapping T; for there is

$$P_{n-1}^* = [T^{-1}(P_n)]^* = T(P_n^*), \quad \text{etc.} \tag{18}$$

Thus, in a certain sense, we can say that $0w$ is an axis of symmetry for the mapping. This is the explanation of the symmetry of the figures (see below, Figs. 3 to 13).

It can be remarked that this symmetry property holds for any mapping which is the product of a mapping and a rotation; in other words, it holds for any mapping similar to (11), with x^2 replaced by an arbitrary function $f(x)$.

b. If α is replaced by $2\pi - \alpha$, (11) shows that T will be replaced by its symmetrical with respect to the $0y$ axis. Thus it is sufficient to consider the range of values $0 \leq \alpha \leq \pi$.

For $\alpha = 0$, T reduces to:

$$x_1 = x, \qquad y_1 = y - x^2, \tag{19}$$

and by iteration, T^n is

$$x_n = x, \qquad y_n = y - nx^2. \tag{20}$$

For $\alpha = \pi$, T^2 is the identity. These two particular cases are trivial and finally we can restrict our attention to the interval

$$0 < \alpha < \pi. \tag{21}$$

c. Let us try to find the invariant points of T, or more generally of T^n. We must solve a system of $2n$ equations for $2n$ unknowns:

$$\begin{aligned} x_{i+1} &= x_i \cos\alpha - (y_i - x_i^2)\sin\alpha, \\ y_{i+1} &= x_i \sin\alpha + (y_i - x_i^2)\cos\alpha, \end{aligned} \qquad (i = 0, \cdots, n-1) \tag{22}$$

with $x_n = x_0$, $y_n = y_0$. The first equation (14) of the inverse mapping gives

$$y_i = (x_{i-1} - x_i \cos\alpha)/\sin\alpha, \tag{23}$$

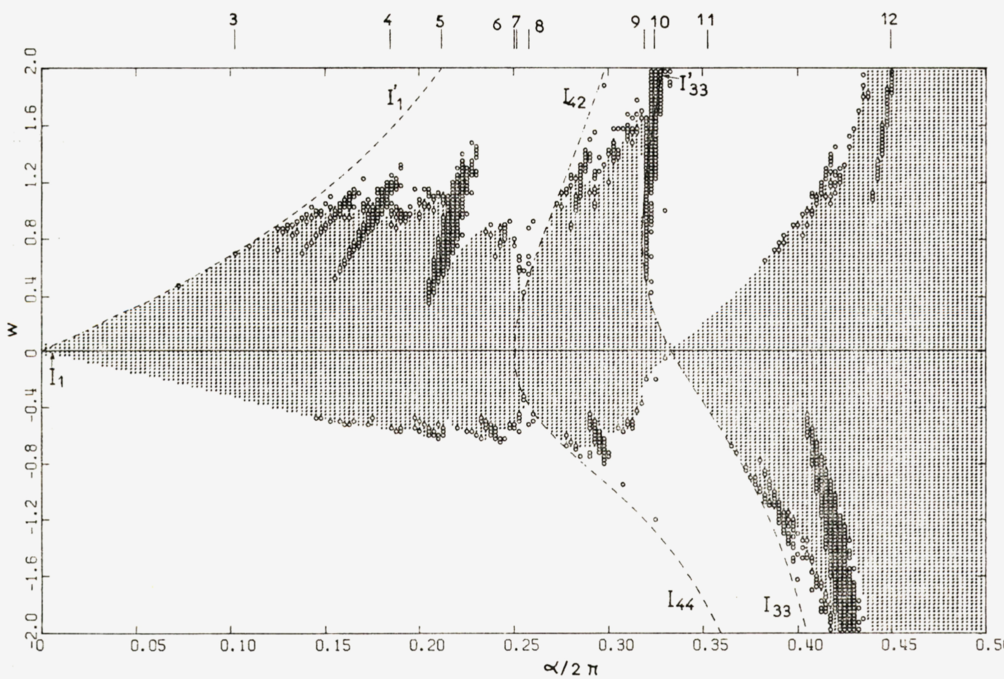

Fig. 2. Summary picture for all values of α, and initial points on the axis of symmetry. Dot: successive points are on a curve. Circle: the points lie on a string of islands. Blank: the points escape, or are scattered. Full curves: stable invariant points. Dashed curves: unstable invariant points. The vertical marks and the numbers above the frame refer to other figures of this paper.

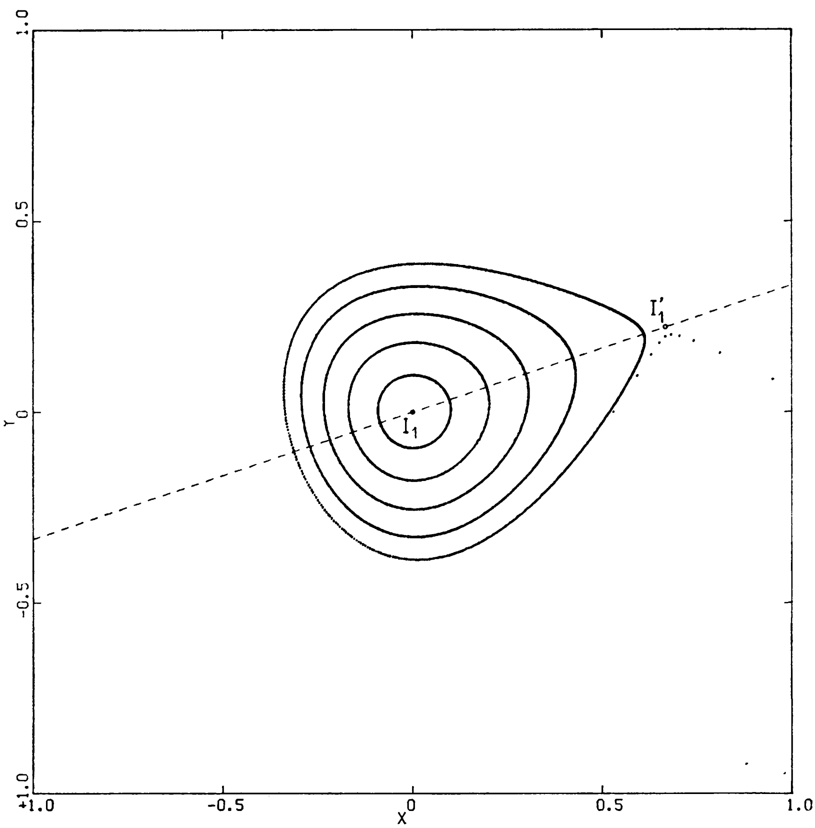

FIG. 3. Structure of the mapping for cos α = 0.8. Sets of points obtained by repeated application of the mapping T for various initial points. Dashed line: axis of symmetry.

and by substitution in the first equation (22) we obtain a system of n equations for n unknowns only:

$$x_i^2 \sin \alpha + 2x_i \cos \alpha - x_{i-1} - x_{i+1} = 0 \qquad (i = 0, \cdots, n-1) \tag{24}$$

with $x_{n-1} = x_{-1}$, $x_n = x_0$. Each equation being of degree 2, the number of solutions will be 2^n at most. (For even values of n, this can also be derived from a more general lemma given by Moser [21].) Explicit computation for $n = 1, 2, 3$, and 4 gives in fact 2, 4, 8, and 16 solutions respectively, as we shall see.

The invariant points of T itself ($n = 1$) are given by (24) with all the x_i's equal. There are two solutions, which we shall call I_1 and I_1'. I_1 is the origin $x = y = 0$. I_1' is given by

$$x = 2 \tan(\alpha/2), \qquad y = 2 \tan^2(\alpha/2). \tag{25}$$

Both I_1 and I_1' are on the axis of symmetry $0w$. I_1 is stable by hypothesis. In order to study the stability of I_1', we displace the origin of coordinates by

$$x = 2 \tan(\alpha/2) + X, \qquad y = 2 \tan^2(\alpha/2) + Y, \tag{26}$$

and the mapping T becomes in the new coordinates:

$$
\begin{aligned}
X_1 &= X\left(\cos\alpha + 4\tan\frac{\alpha}{2}\sin\alpha\right) - Y\sin\alpha + X^2\sin\alpha, \\
Y_1 &= X\left(\sin\alpha - 4\tan\frac{\alpha}{2}\cos\alpha\right) + Y\cos\alpha - X^2\cos\alpha.
\end{aligned}
\tag{27}
$$

The trace of the matrix of the first-order coefficients is

$$(\cos\alpha + 4\tan(\alpha/2)\sin\alpha) + \cos\alpha = 2 + 4\sin^2(\alpha/2). \tag{28}$$

According to (21), this is always greater than 2; hence I_1' is always unstable.

A similar computation shows that T^2 has four invariant points. Two of them are I_1 and I_1', already known; the two other ones, which we shall call I_{21} and I_{22}, are associated in the following way:

$$I_{22} = T(I_{21}), \qquad I_{21} = T(I_{22}). \tag{29}$$

They have complex coordinates:

$$
\begin{aligned}
x &= -\cot(\alpha/2) \pm i(1 + 1/\sin^2(\alpha/2))^{1/2}, \\
y &= -1 \mp i\cot(\alpha/2)(1 - 1/\sin^2(\alpha/2))^{1/2},
\end{aligned}
\tag{30}
$$

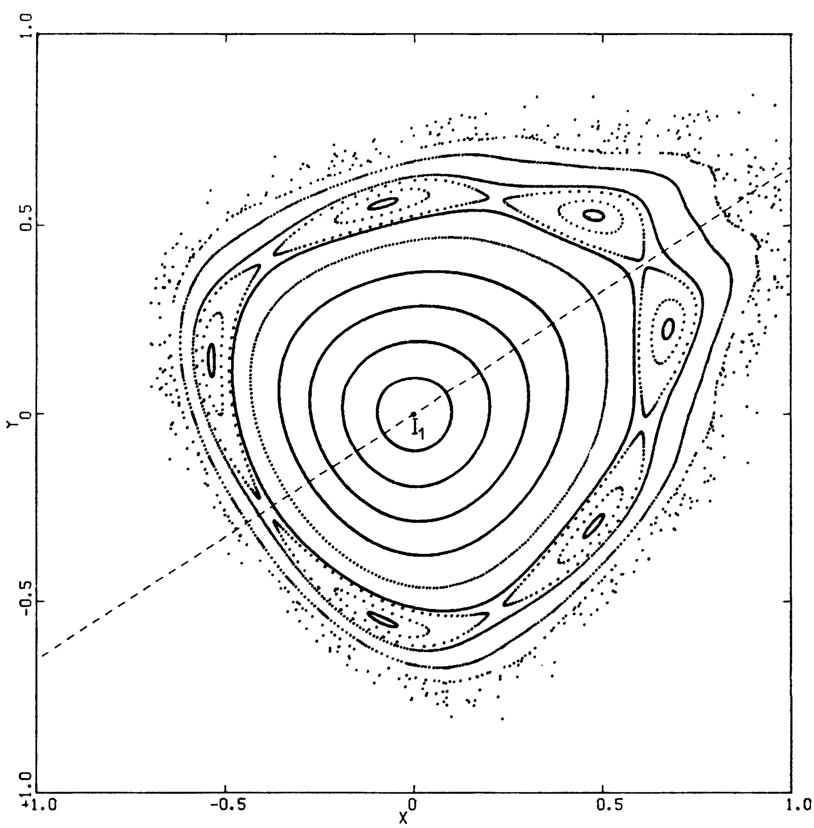

FIG. 4. $\cos\alpha = 0.4$.

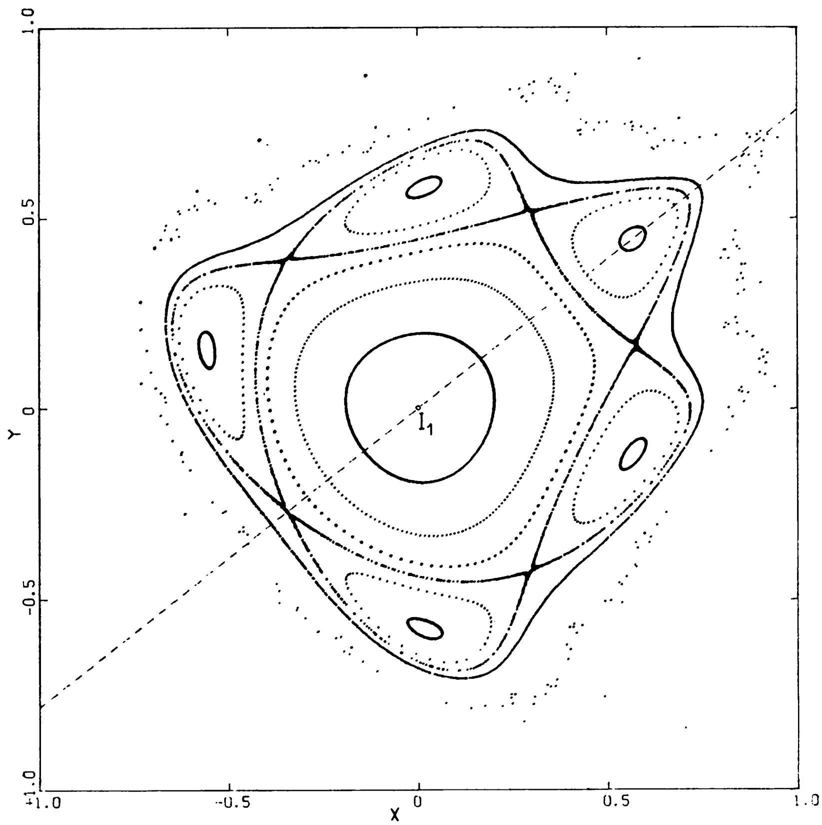

FIG. 5. $\cos \alpha = 0.24$.

with $i = (-1)^{1/2}$; thus they are not of immediate interest to us since we consider the mapping T only for real values of x and y.

T^3 has eight invariant points. Two of them are again I_1 and I_1'. The other six, which we shall call I_{31}, I_{32}, I_{33}, I_{31}', I_{32}', I_{33}', are associated in two groups of three in the following way:

$$I_{32} = T(I_{31}), \qquad I_{33} = T(I_{32}), \qquad I_{31} = T(I_{33}), \tag{31}$$

and similarly for I_{31}', I_{32}', I_{33}'. Their coordinates are

$$\begin{aligned}
x_{31} &= [-(1 + \cos \alpha) + Q]/\sin \alpha, \\
y_{31} &= [\cos^2 \alpha - (1 + \cos \alpha)Q]/\sin^2 \alpha, \\
x_{32} &= [-\cos \alpha - Q]/\sin \alpha, \\
y_{32} &= [\cos^2 \alpha - \cos \alpha - 1 + (1 + \cos \alpha)Q]/\sin^2 \alpha, \\
x_{33} &= [-\cos \alpha - Q]/\sin \alpha, \\
y_{33} &= [\cos^2 \alpha - \cos \alpha + (\cos \alpha - 1)Q]/\sin^2 \alpha,
\end{aligned} \tag{32}$$

with

$$Q = \pm(\cos^2 \alpha - 2 \cos \alpha - 1)^{1/2}, \tag{33}$$

with the plus sign for the first group and the minus sign for the second group. The expression (33), and therefore the six invariant points, are real only if

$$\cos \alpha \leq 1 - 2^{1/2}. \tag{34}$$

We shall not reproduce the stability computation, which is tedious but straightforward. The result is that inside the domain of reality (34), the points I_{31}, I_{32}, I_{33} are always unstable; the points I'_{31}, I'_{32}, I'_{33} are stable for $-\frac{1}{2} < \cos \alpha < 1 - 2^{1/2}$, and unstable for $-1 < \cos \alpha \leq -\frac{1}{2}$.

T^4 has sixteen invariant points. Four of them are I_1, I'_1, I_{21}, I_{22}. The other twelve are associated in three groups of four in the following way:

$$I_{42} = T(I_{41}), \qquad I_{43} = T(I_{42}), \qquad I_{44} = T(I_{43}), \qquad I_{41} = T(I_{44}), \tag{35}$$

and similarly for I'_{41}, I'_{42}, I'_{43}, I'_{44}, and I''_{41}, I''_{42}, I''_{43}, I''_{44}. The coordinates for the first group are

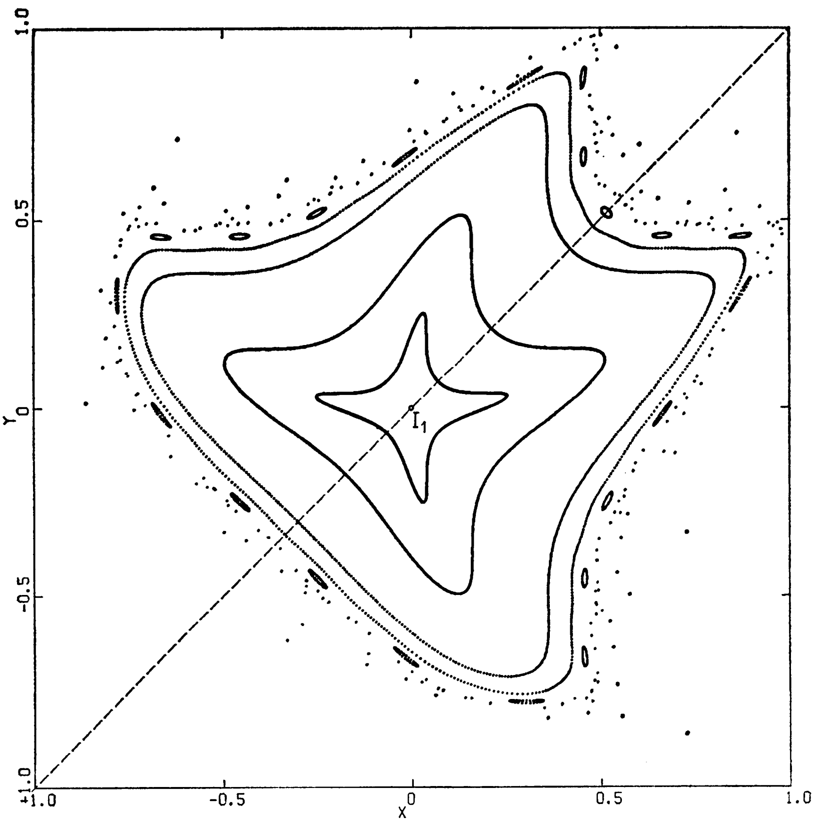

FIG. 6. $\cos \alpha = 0$.

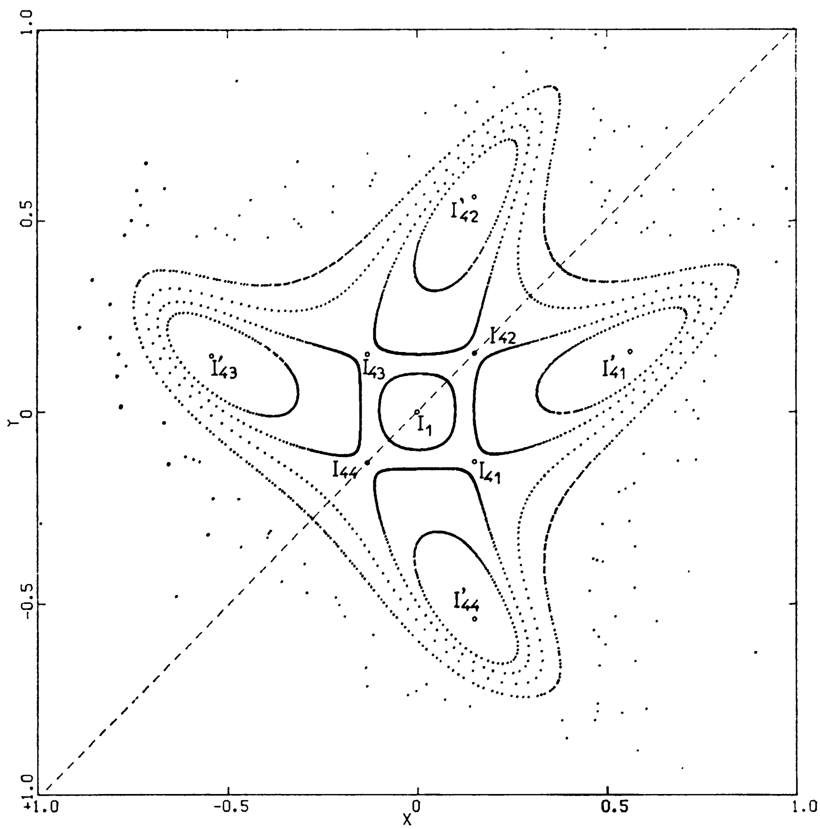

FIG. 7. $\cos\alpha = -0.01$.

$$
\begin{aligned}
x_{41} &= [-\cos\alpha + Q']/\sin\alpha,\\
y_{41} &= [\cos^2\alpha - \cos\alpha - (\cos\alpha + 1)Q']/\sin^2\alpha,\\
x_{42} &= [-\cos\alpha + Q']/\sin\alpha,\\
y_{42} &= [\cos^2\alpha - \cos\alpha + (1 - \cos\alpha)Q']/\sin^2\alpha,\\
x_{43} &= [-\cos\alpha - Q']/\sin\alpha,\\
y_{43} &= [\cos^2\alpha - \cos\alpha + (\cos\alpha + 1)Q']/\sin^2\alpha,\\
x_{44} &= [-\cos\alpha - Q']/\sin\alpha,\\
y_{44} &= [\cos^2\alpha - \cos\alpha + (\cos\alpha - 1)Q']/\sin^2\alpha,
\end{aligned}
\tag{36}
$$

with

$$Q' = (\cos^2\alpha - 2\cos\alpha)^{1/2}. \tag{37}$$

These points are real for

$$\cos\alpha \le 0. \tag{38}$$

Stability analysis shows that they are always unstable.

The coordinates for the second group are

$$\begin{aligned}
x'_{41} &= [-\cos\alpha + Q'']/\sin\alpha, \\
y'_{41} &= [\cos^2\alpha - \cos\alpha + Q' - Q''\cos\alpha]/\sin^2\alpha, \\
x'_{42} &= [-\cos\alpha + Q']/\sin\alpha, \\
y'_{42} &= [\cos^2\alpha - \cos\alpha + Q'' - Q'\cos\alpha]/\sin^2\alpha, \\
x'_{43} &= [-\cos\alpha - Q'']/\sin\alpha, \\
y'_{43} &= [\cos^2\alpha - \cos\alpha + Q' + Q''\cos\alpha]/\sin^2\alpha, \\
x'_{44} &= [-\cos\alpha + Q']/\sin\alpha, \\
y'_{44} &= [\cos^2\alpha - \cos\alpha - Q'' - Q'\cos\alpha]/\sin^2\alpha,
\end{aligned} \tag{39}$$

with

$$Q'' = (Q'^2 + 2Q')^{1/2}. \tag{40}$$

The domain of reality of these points is again given by (38). Inside that domain, they are stable for

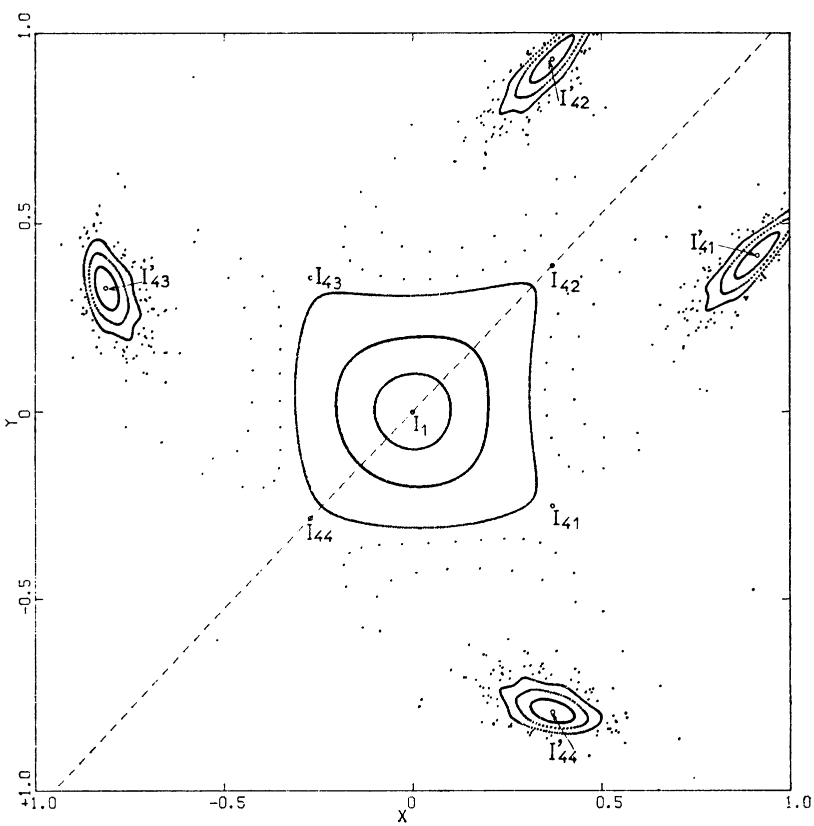

FIG. 8. $\cos\alpha = -0.05$.

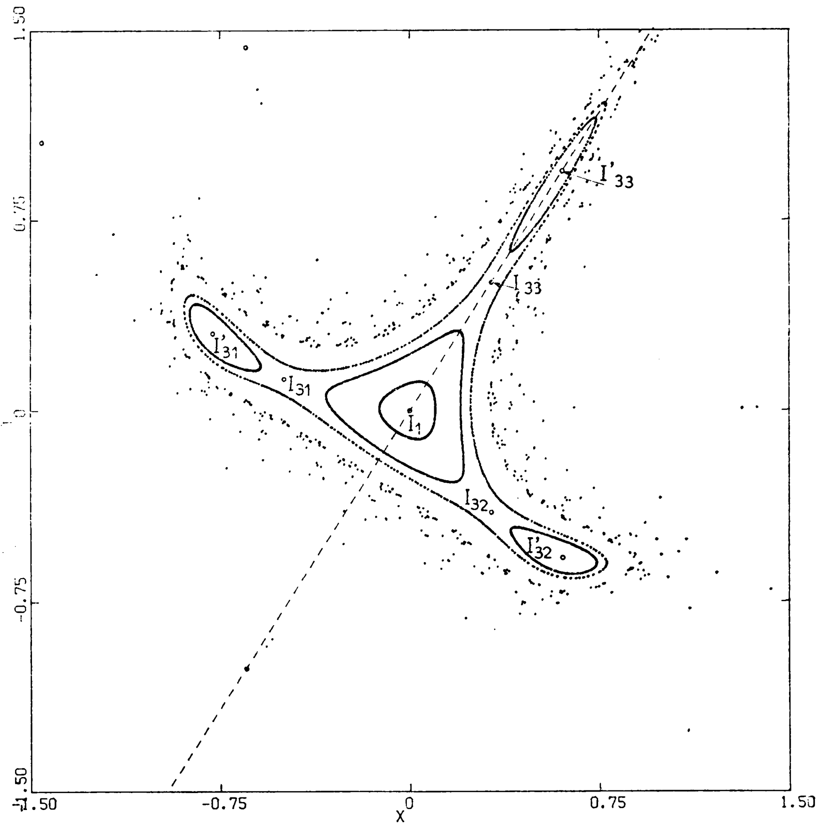

FIG. 9. $\cos \alpha = -0.42$.

$$Q'^2(Q'^2 + 2Q') < \tfrac{1}{4}, \tag{41}$$

that is,

$$\cos \alpha_0 = -0.10336015 \cdots < \cos \alpha < 0, \tag{42}$$

and they are unstable for $-1 < \cos \alpha \leq \cos \alpha_0$.

The last group is given by the same formulas (39) and (40), but replacing Q' by $-Q'$. These points are never real and thus can be neglected.

For $n > 4$, it does not seem possible to solve the system (24) explicitly. The solutions could be found numerically, but we have not attempted it in view of their lesser importance. T^5 has probably 32 invariant points, of which 2 are I_1 and I_1', the others forming 6 groups of 5; similarly, T^6 has probably 64 invariant points, of which 10 are I_1, I_1', I_{21}, I_{22}, I_{31}, I_{32}, I_{33}, I_{31}', I_{32}', I_{33}', the others forming 9 groups of 6; and so on.

d. At great distances from the origin, quadratic terms become dominant in the equations of the mapping (11) and there is approximately

$$x_{i+1} \approx x_i^2 \sin \alpha; \tag{43}$$

hence,

$$x_{i+j} \sin \alpha \approx (x_i \sin \alpha)^{2^j}. \tag{44}$$

If $|x_i| > 1/\sin \alpha$, then $x_{i+j} \to +\infty$ for $j \to +\infty$: the successive points "escape" to infinity. Once started, this escape motion accelerates very quickly, because of the exponent 2^j: the distance to the origin is roughly squared by every application of the mapping.

4. Numerical results. For most physical systems with two degrees of freedom, a problem of great practical importance is the ultimate behaviour of the solutions after a very long time, or mathematically speaking, for $t \to +\infty$. Formulated in terms of the associated mapping, this problem becomes: given an initial point P_0, what are the properties of the set of points obtained by repeated application of the mapping:

$$P_0\,,\ P_1 = T(P_0)\,,\ \cdots\,,\ P_n = T^n(P_0)\,,\ \cdots\ ? \tag{45}$$

This problem lends itself very well to numerical experiments: up to 10^6 successive points can be computed, if needed, in a reasonable time. In fact, experience shows that a much smaller number of points (100 to 1000) is sufficient in most cases to determine the properties of the set (45) with a fair amount of reliability. The great speed of the computer can then be used to explore in detail the variations of these properties with the position of the initial point P_0 and with the parameter α. A great quantity of data can be accumulated in this way; only a sample of the results will be presented here.

As a first illustrative example, consider Fig. 4. It shows some typical sets of points obtained by numerical computation, for a given value of the parameter α: $\cos \alpha = 0.4$,

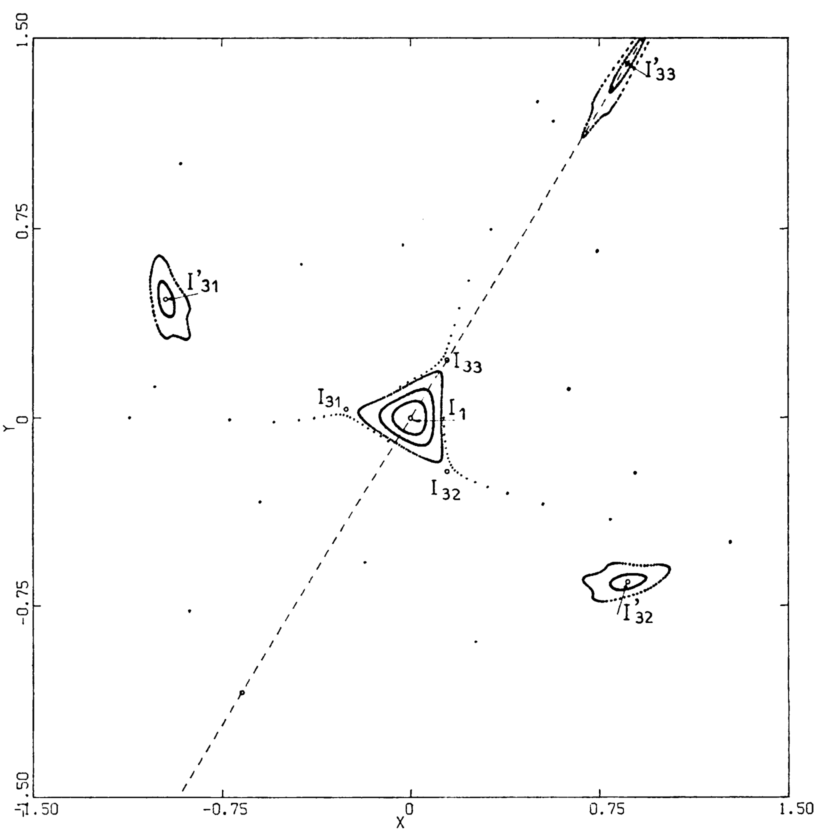

FIG. 10. $\cos \alpha = -0.45$.

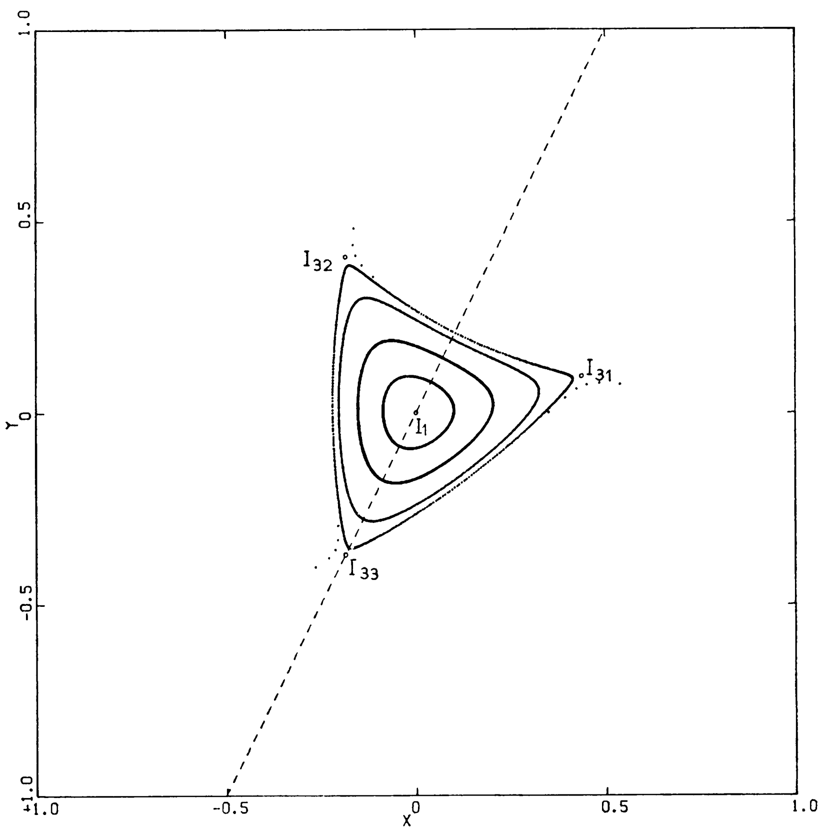

FIG. 11. cos α = −0.60.

and for different initial points (see Table 1). The dashed line is the axis of symmetry. This picture exhibits all the characteristic and well-known features of problems with two degrees of freedom [3, 15]; we shall describe them briefly. In many cases, the set of points seems to lie exactly on a closed curve surrounding the origin. (In some cases the points are so dense that they cannot be distinguished and give in fact the illusion of a continuous curve.) This curve is almost circular near the origin; this is easily explained if one considers the first-order terms in (11). For increasing dimensions, the curve becomes more and more distorted, until at some point there is a sudden break-up and the set of points no longer lies on a curve, but seems rather to fill some region in the plane; this is the case for the outermost set of points on Fig. 4. In fact, after approximately 650 iterations of the mapping, the points of this set go out of the frame and escape to infinity by the mechanism described above (Sec. 3d). Experience shows that this behaviour is typical and that scattered sets of points almost always escape to infinity in the end.

On each curve, the arrangement of the points is topologically the same as if the mapping were a simple rotation by a given angle ω. This property is not apparent on Fig. 4, but can be verified by a detailed examination of the coordinates of the successive points. ω is called the *rotation number* of the curve. It has different values for different curves, and seems to change in a continuous way with the dimensions of the curve. When the dimensions shrink to nothing and the curve reduces to the origin, $\omega \to \alpha$; this again is obvious from the first-order terms in (11).

When $\omega/2\pi$ goes through a rational value m/n, with m and n integers, the curve breaks into a string of n closed curves or "islands"; one conspicuous example can be seen on Fig. 4, corresponding to $m = 1$ and $n = 6$. Inside each island, there is a stable invariant point of T^n, and between two neighbouring islands, where they almost join, there is an unstable invariant point of T^n. Successive points jump from one island to another by application of the mapping. If we consider T^n as the elementary mapping instead of T, each island will present the same structure, on a reduced scale, as the whole mapping; in particular it will contain second-order islands, and so on, so that the whole picture is of incredible complexity.

These features are predicted by the theory, at least in a qualitative way. For example, the existence of invariant curves around the origin has been proved [13, 14], but only in a very small region around the origin, with dimensions of the order of 10^{-48}[2]. The strings of islands can also be explained [15]. But the sudden disappearance of the curves past a certain distance from the origin has not yet received a satisfactory explanation, although some possible mechanisms have been suggested [2, 11, 16, 17]. This drastic change in the properties of the set of points is of course of great importance in all applications.

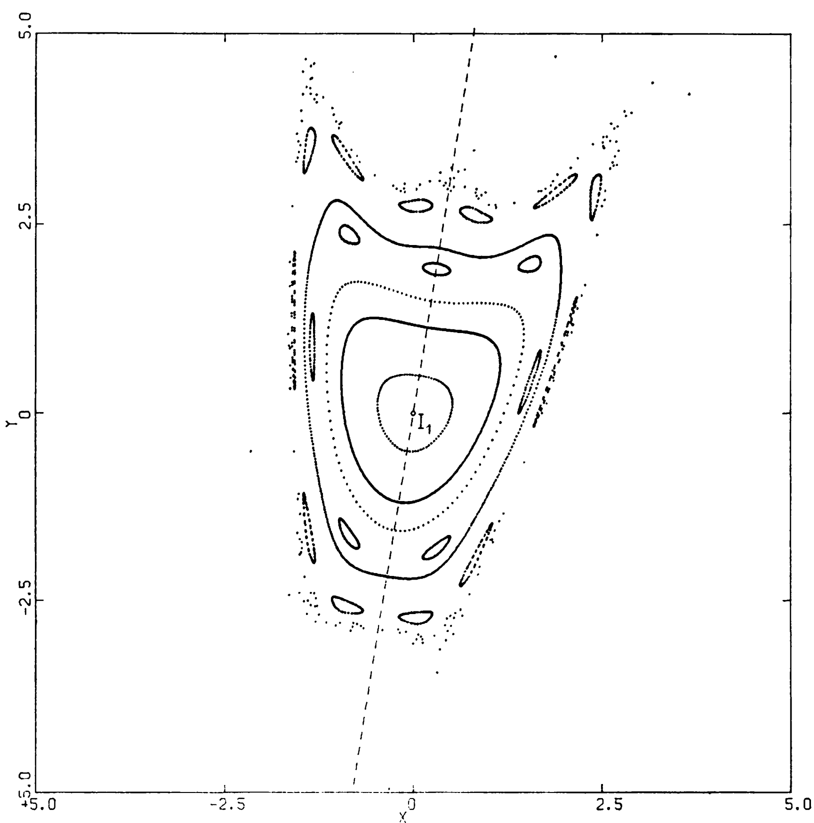

Fig. 12. $\cos \alpha = -0.95$.

It should be pointed out here that the divergence of Birkhoff's transformation [10] has been rigorously proven by Moser [21] for a class of mappings which includes the quadratic mapping studied here.

The series of Figs. 3 to 12 shows how the structure of the mapping evolves when α goes from 0 to π. Table 1 gives the coordinates x_0, y_0 of the initial points, and the number n of successive points computed and displayed. One word of caution is necessary here for the reader who might eventually want to duplicate these results. Sets of points lying on curves or on islands should be accurately reproducible on any computer from the parameters given in Table 1; for the sets of scattered points, on the other hand, one should not expect exact reproduction, because these sets are by nature extremely divergent [3]: any error, however small, in the position of a point, is exponentially amplified by repeated application of the mapping and soon results in completely different positions of individual points. Small errors necessarily arise from the rounding-off procedure of the computer.

Fig. 2 is a summary picture and shows a cross-section of the mapping along its axis of symmetry, as a function of α. The vertical marks above the frame indicate the particular values of α for which the full mapping is represented, on Figs. 3 to 12. Fig. 2 has been obtained as follows: for every couple of values $\alpha/2\pi = 0.0025(0.0025)0.4975$ and $w = -1.975(0.025)1.975$, starting from the point with abscissa w on the $0w$ axis, 100 successive points are computed by repeated application of the mapping. If the points lie on a curve, a dot is inscribed on Fig. 2 at the appropriate location. If the points are on a string of islands, a little circle is inscribed. If the points are scattered, or escape, nothing is inscribed. A special computer program was set up for the automatic discrimination of curves, islands, and scattered points; it uses essentially the angular positions of successive points with respect to the origin. Escape was considered to take place as soon as a point went farther than a given distance from the origin ($r_{\max} = 1000$).

With the computer used (IBM 7040), the mean computing time for one application of the mapping is about 2 milliseconds, and the total computing time for the production of Fig. 2 was about 1 hour. The computations were made in most cases with an accuracy of 16 decimal digits.

The invariant points I_1, I_1', I_{33}, I_{33}', I_{42}, I_{44}, which lie on the axis of symmetry $0w$, are also represented on Fig. 2; they appear as curves, whose equations are given by (25), (32), and (36). Full lines indicate stable points; dashed lines, unstable points.

For small values of α, the region of curves seems to be limited by the unstable invariant point I_1', as is shown by Fig. 3, and also quite convincingly by Fig. 2. The set of isolated points at the right of Fig. 3 shows how this happens: in the vicinity of the unstable invariant point, successive points lie approximately on arcs of hyperbolas having I_1' as center. Thus, past a certain dividing line, the points bifurcate towards the right instead of the left, and escape.

For $\alpha \to 0$, $I_1' \to I_1$, and the curve region shrinks to nothing.

As α increases, we encounter cases where the boundary of the curve region is not so well defined, and cannot be associated with unstable invariant points in any obvious way; this is the case for Fig. 4. The limit of the points becomes fuzzy on Fig. 2.

Fig. 5 exhibits a string of 5 large islands. One of the islands is situated on the positive $0w$ axis; this explains the large band on Fig. 2. The same Fig. 2 shows that these islands move away from the center and grow larger when α increases; they are first inside the curve region (this is the case for Fig. 5), then outside. Similar bands appear on Fig. 2

TABLE 1

Data for Figs. 3 to 14.

Fig.	cos α	x_0	y_0	n	comments
3	0.8	0.1	0.	196	
		0.2	0.	282	
		0.3	0.	422	
		0.41	0.	542	
		0.52	0.	645	
		0.53	0.	14	escape
4	0.4	0.1	0.	200	
		0.2	0.	360	
		0.3	0.	840	
		0.4	0.	871	
		0.5	0.	327	
		0.58	0.	1164	
		0.61	0.	1000	6 islands
		0.63	0.2	180	6 islands
		0.66	0.22	500	6 islands
		0.66	0.	694	
		0.73	0.	681	
		0.795	0.	657	escape
5	0.24	0.2	0.	651	
		0.35	0.	187	
		0.44	0.	1000	
		0.60	−0.1	1000	5 islands
		0.68	0.	250	5 islands
		0.718	0.	3000	scattered points
		0.75	0.	1554	
		0.82	0.	233	escape
6	0.	0.2	0.	1332	
		0.4	0.	1422	
		0.6	0.	697	
		0.65	0.	621	
		0.68	0.	1000	21 islands
		0.70	0.	255	escape
7	−0.01	0.1	0.	182	
		0.15	0.	1500	4 islands
		0.35	0.	500	4 islands
		0.54	0.	210	
		0.59	0.	437	
		0.68	0.	157	escape
8	−0.05	0.1	0.	224	
		0.2	0.	1508	
		0.31	0.	561	
		0.32	0.9	500	4 islands
		0.30	0.9	500	4 islands
		0.28	0.9	1000	4 islands
		0.26	0.9	460	escape

TABLE 1 (*Continued*)

9	−0.42	0.1	0.	340	
		0.2	0.	528	
		0.24	0.	1000	
		0.32	0.	729	escape
		0.6	1.	550	3 islands
10	−0.45	0.06	0.	200	
		0.09	0.	254	
		0.12	0.	176	
		0.13	0.	76	escape
		0.88	1.4	500	3 islands
		0.90	1.4	500	3 islands
11	−0.60	0.1	0.	306	
		0.2	0.	1616	
		0.3	0.	608	
		0.34	0.	602	
		0.35	0.	34	escape
12	−0.95	0.5	0.	84	
		1.	0.	502	
		1.2	0.	121	
		1.4	0.	500	7 islands
		1.5	0.	512	
		1.65	0.	1000	12 islands
		1.71	0.	194	escape
13	0.22	0.83	0.	2000	scattered points
		0.7	0.	1000	5 islands
14	0.24	0.55	0.16	10000	
		0.565	0.16	10000	
		0.569	0.16224	10000	
		0.718	0.	50000	scattered points
		0.57	0.11	10000	5 islands
		0.57	0.12	10000	5 islands
		0.57	0.125	10000	second-order islands
		0.57	0.13	10000	third-order islands
		0.5905	0.163	10000	76 islands
		0.598	0.157	10000	71 islands
		0.602	0.16	10000	66 islands
		0.610	0.16	10000	61 islands
		0.615	0.16	10000	
		0.620	0.16	10000	56 islands

for smaller values of α; they correspond to strings of 7 and 9 islands. The chain of 6 islands of Fig. 4 does not appear on Fig. 2 because none of the islands is on the axis of symmetry. (Incidentally, it seems that all strings with an even number of islands possess this property, namely, the centers of the islands are never on the axis of symmetry. We have not been able to find an explanation for this observed fact.)

$\alpha/2\pi = \frac{1}{4}$ (Fig. 6) is a particular case: the curves near the origin are no more circular, but are made approximately of four branches of hyperbolas, truncated and linked together at some distance. This phenomenon has been theoretically explained [18].

For $\alpha/2\pi$ a little greater than $\frac{1}{4}$, two groups of invariant points of T^4 appear (Fig. 7; see Sec. 3c). One of these groups is stable and gives rise to very large islands. These islands are first inside the curve region, then outside (Fig. 8). In this last case, the curve region appears to be limited by the four unstable invariant points I_{41} to I_{44} ; this is confirmed by an examination of Fig. 2.

For $\cos \alpha < 1 - 2^{1/2}$, two groups of invariant points of T^3 appear (see Sec. 3c). One of them is stable and gives rise to three islands, which again are first inside the curves (Fig. 9), then outside (Fig. 10). (Note the change of scale for these two figures.) One of the islands, on the positive $0w$ axis, produces a band on Fig. 2. The peculiar disposition of the unstable invariant points I_{31} , I_{32} , I_{33} should be noted: instead of lying between successive islands, they are placed between each island and the origin.

$\alpha/2\pi = \frac{1}{3}$ is another particular case, for which it is known that no invariant curves exist in general [18]; this has been explicitly shown for the present mapping by Siegel [12]. Figures 2, 10, 11 show that the curve region, in the vicinity of this particular value, is limited by the three unstable invariant points I_{31} , I_{32} , I_{33} . These points go through

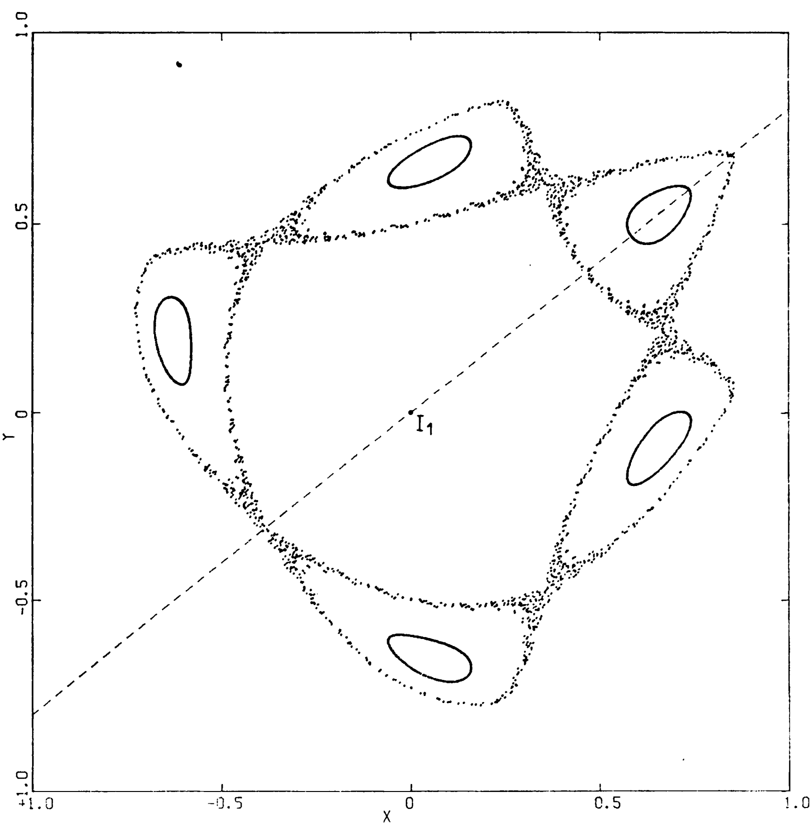

FIG. 13. $\cos \alpha = 0.22$: a scattered set surrounding five islands.

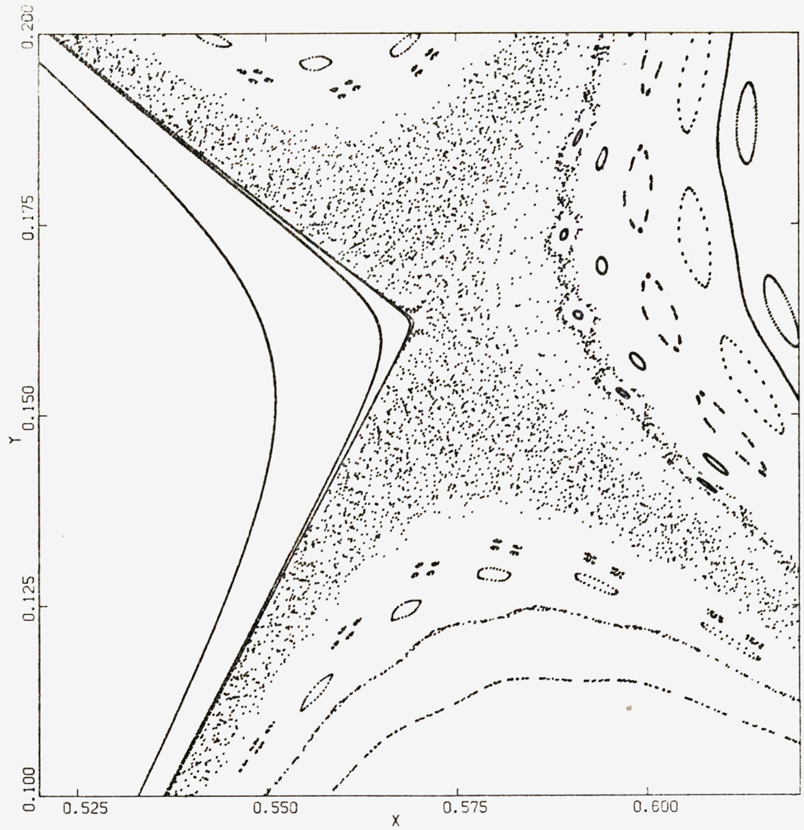

FIG. 14. $\cos\alpha = 0.24$: enlargement of the vicinity of an unstable invariant point of T^5.

the origin when $\alpha/2\pi$ goes through the value $\frac{1}{3}$, as shown by Eqs. (32); this causes the triangle-shaped curve region to shrink to nothing and then to invert its shape. Examples of sets escaping along hyperbolic lines can be seen on Figs. 10 and 11.

Finally, for $\alpha \to \pi$, the curve region becomes larger and larger and tends to cover the whole plane (Fig. 12; note the change of scale). It becomes also more and more elongated in the direction of the axis of symmetry. Two sets of 7 and 12 islands can be seen on Fig. 12; the set of 7 islands gives rise to a band on Fig. 2.

It has been already remarked that every island has essentially the same structure as the whole mapping, on a reduced scale. In particular, we should expect that past a given distance from the center of the island, the points will be scattered. This is in fact what happens; an example is shown on Fig. 13. Each island is surrounded by a region of scattered points, and it can be seen that these regions join together in the vicinity of the unstable invariant points, where there is an accumulation of points. 2000 successive points have been represented in the set of Fig. 13; by a prolonged computation it was found that the points escape after 2478 applications of the mapping.

A similar case can be seen in Fig. 5, although the scattering is not so clearly visible. This case is more interesting because there exist invariant curves surrounding the five islands, so that the scattered set cannot escape to infinity: it is constrained to remain in a finite region of the plane, limited by an inner curve, an outer curve, and the islands. Fig. 14 shows a 20-fold enlargement of the vicinity of an unstable invariant point; initial conditions are given in Table 1. All scattered points in this picture belong to the same set, for which 50,000 successive points have been computed. They fill a given region of the plane, in a fairly uniform fashion.

On the left of Fig. 14, points appear to lie exactly on curves, and these curves seem to approach the unstable invariant point (which has the coordinates $x = 0.56963267 \cdots$, $y = 0.16224047 \cdots$) very closely; by further enlargements it was found that the curves break only at a distance of the order of 10^{-5} from the invariant point. On the right, the behaviour is strikingly different: the points appear to degenerate into strings of islands in most cases. The border of the set of scattered points is not well defined. It can be remarked that the innermost set of small islands is inside the region of scattered points. At the top and bottom of Fig. 14 can be seen pieces from two of the five large islands of Fig. 5, and in particular an instance of second-order islands, and another one of third-order islands. Here again the limit of the set of scattered points is not well defined.

5. Conclusions. It has been shown that the very simple mapping given by the formulas (11) gives rise to a remarkable variety of shapes, and apparently has all the typical properties of more complicated problems of the same kind. Therefore it appears as a good model for the general study of dynamical systems with two degrees of freedom. In the present paper, we have limited ourselves to a description of the main properties of the mapping. In another paper [11], this mapping has been used for the study of a specific question, namely: can Birkhoff's divergent series be used to find the invariant curves, and in particular the limit of their region of existence? Similarly, the mapping (11) could be used to study other questions arising either from the theory or from the needs of particular applications.

References

[1] M. Henon, *Exploration numérique du problème restreint.* I, II, Ann. Astrophys. **28**, 499–511 and 992–1007 (1965)

[2] M. Henon, *Exploration numérique du problème restreint.* III, IV, Bull. Astron. (série 3) **1**, fasc. **1**, 57–79 and fasc. 2, 49–66 (1966)

[3] M. Henon and C. Heiles, *The applicability of the third integral of motion: some numerical experiments,* Astronom. J. **69**, 73–79 (1964)

[4] W. T. Kyner, *Qualitative properties of orbits around an oblate planet,* Comm. Pure Appl. Math. **17**, 227–236 (1964)

[5] V. A. Zlatoustov, D. E. Okhotsimskii, V. A. Sarychev, A. P. Torzhevskii, *Oscillations of a satellite in the plane of an elliptic orbit,* Kosmicheskie Issledovaniya **2**, 657–666 (1964) (Russian)

[6] A. J. Dragt, *Trapped orbits in a magnetic dipole field,* Rev. Geophys. **3**, 255–298 (1965)

[7] A. Garren, R. J. Riddell, L. Smith, G. Bing, L. R. Henrich, T. G. Northrop, J. E. Roberts, *Individual particle motion and the effects of scattering in an axially symmetric magnetic field,* Proc. Second U. N. International Conf. on Peaceful Uses of Atomic Energy (United Nations, Geneva) **31**, 65–71 (1958)

[8] T. G. Northrop, *The adiabatic motion of charged particles,* Interscience Publishers, New York, 1963, Chap. 5

[9] G. D. Birkhoff, *Dynamical systems with two degrees of freedom,* Trans. Amer. Math. Soc. **18**, 199–300 (1917)

[10] G. D. Birkhoff, *Surface transformations and their dynamical applications,* Acta Math. 43, 1–119 (1920)

[11] J. Roels and M. Henon, *Recherche des courbes invariantes d'une transformation ponctuelle plane conservant les aires,* Bull. Astronom. (série 3) **2**, 267–285 (1967)

[12] C. L. Siegel, *Vorlesungen über Himmelsmechanik,* Springer-Verlag, Berlin, 1956, p. 203

[13] V. I. Arnol'd, *Proof of a theorem of A. N. Kolmogorov on the invariance of quasi-periodic motions*

under small perturbations of the Hamiltonian, Uspehi mat. Nauk **18**, no. 5, 13–40 = Russian Math. Surveys **18**, no. 5, 9–36 (1963)

[14] J. Moser, *On invariant curves of area-preserving mappings of an annulus*, Nachr. Akad. Wiss. Göttingen, Math.-Phys. Kl., no. 1, 1–20 (1962)

[15] V. I. Arnold and A. Avez, *Problèmes ergodiques de la mécanique classique*, Gauthier-Villars, Paris, 1967

[16] G. Contopoulos, *Resonance phenomena and the nonapplicability of the "third" integral*, Bull. Astronom. (série 3) **2**, 223–241 (1967)

[17] B. V. Chirikov, *When does the dynamical system turn into the statistical one?*, Comm. at the International Congress of Mathematicians, Moscow, 1966

[18] J. Moser, *Stability of the asteroids*, Astronom. J. **63**, 439–443 (1958)

[19] W. Engel, *Ein Satz über ganze Cremona-Transformationen der Ebene*, Math. Ann. **130**, 11–19 (1955)

[20] W. Engel, *Ganze Cremona-Transformationen von Primzahlgrad in der Ebene*, Math. Ann. **136**, 319–325 (1958)

[21] J. Moser, *On the integrability of area-preserving Cremona mappings near an elliptic fixed point*, Bol. Soc. Mat. Mexicana, 176–180 (1960)